ELSEVIER

Earth and Planetary Science Letters 186 (2001) 497–512

EPSL

www.elsevier.com/locate/epsl

Tracing Papua New Guinea imprint on the central Equatorial Pacific Ocean using neodymium isotopic compositions and Rare Earth Element patterns

F. Lacan, C. Jeandel *

LEGOS (CNRS/CNES/UPS), Observatoire Midi-Pyrénées, 14, Ave E. Belin, F-31400 Toulouse, France

Received 29 September 2000; received in revised form 29 January 2001; accepted 4 February 2001

Abstract

The Nd isotopic composition (IC) and Rare Earth patterns of hydrodynamic structures of the Equatorial Pacific Ocean were characterized along 140°W. The Nd IC of Antarctic Intermediate Water (AAIW) and of the lower layer of the Equatorial Undercurrent (EUC) at 140°W (13°C Water) are much more radiogenic at the equator than at their origin in the South Equatorial Current (12°S), revealing that these water masses have been in contact with the highly radiogenic Papua New Guinea (PNG) slope. In both cases, only a small fraction (less than 9%) of the sediment deposited on the PNG slope is required to be exchanged or dissolved to explain these Nd IC variations, whereas the hydrographic properties of the same water masses remain unchanged. This confirms the usefulness of this tracer to identify pathways of water masses. These results emphasize the importance of jets in transporting lithogenic material into the subsurface layers of remote areas, where aeolian inputs are particularly weak and corroborate the previous results on Fe and Al maximum in this area [M.L. Wells, G.K. Vallis, E.A. Silver, Nature 398 (1999) 601–604]. The Nd IC of the upper layer of the EUC contrasts strongly to that of the subpycnocline layer, indicating that the equatorial upwelling only affects the surface waters and is not effective between 120 and 150 m. We calculate that the Nd imprint of the PNG input is likely to vanish from this surface layer as it traverses the basin, due to the replacement of upwelled waters by non-radiogenic ones.

Keywords: neodymium; isotopic composition; rare earths; sea water; geochemical indicators; Papua New Guinea

1. Introduction

Since the eighties, the neodymium isotopic composition (Nd IC) of sea water has been recognized as a tracer in marine geochemistry. The Nd IC corresponds to the $^{143}Nd/^{144}Nd$ ratio. It is expressed as ε_{Nd} which is the deviation of this ratio from its average value in the earth:

$$\varepsilon_{Nd} = \left(\frac{\left(\frac{^{143}Nd}{^{144}Nd}\right)_{measured}}{\left(\frac{^{143}Nd}{^{144}Nd}\right)_{CHUR}} - 1 \right) \times 10^4$$

The present-day $^{143}Nd/^{144}Nd$ ratio in the CHUR (Chondritic Uniform Reservoir) taken as reference is 0.512638 [2]. In the ocean, dissolved

E-mail: francois.lacan@cnes.fr

* Corresponding author. Tel.: +33-5-6133-29033; Fax: +33-5-6125-3205; E-mail: catherine.jeandel@cnes.fr

0012-821X/01/$ – see front matter
PII: S0012-821X(01)00263-1

ε_{Nd} values allow the pathways and mixing of water masses on the oceanic basin scale to be traced [3–7]. In contrast to many circulation tracers, the sea water Nd IC is not affected by evaporation or any subtraction processes: the ε_{Nd} of any given water mass will only be modified when it receives an input of Nd with a different isotopic signal. Therefore, modification of the isotopic signature of a water body implies mixing with other water bodies and/or contact and exchange with continental inputs [7–9]. The Nd IC is also a powerful tracer of the sources and fates of marine particles: as Nd is a lithogenic element, it is brought to the sea by continental inputs. The distribution of ε_{Nd} in the solid earth is heterogeneous, varying from −36 for old granitic cratons to more than +10 for recent Mid Ocean Ridge Basalts (see the compilation in the data bank www.earthref.org). Therefore, pathways of particles between their sampling location and their source can be reconstructed and transformation processes through the water column can also be studied using ε_{Nd} ([10,11] and references therein, [12,13]).

In addition to its isotopic properties, Nd belongs to the geochemical group of the Rare Earth Elements (REE). In the ocean, the dissolved REE distribution is determined by the competition between soluble carbonate–REE(III)$^+$ complexes and the removal of REE(III)$^+$ by particle scavenging [14]. This competition causes fractionation between light and heavy REE (LREE and HREE). Moreover, cerium, which is oxidized to insoluble Ce(IV)$^+$, is removed more effectively than its REE neighbors. These fractionations are represented by the REE pattern, that is all the REE concentrations measured in a sample normalized using the REE data of a reference material. This is a useful tool to identify which marine process could have modified the distribution of the REE in sea water (adsorption, desorption, redox process..., [14–16] and references therein). The simultaneous use of both the Nd IC and REE patterns is a fruitful approach for analyzing the dissolved/particulate exchanges and pathways of particles in sea water [13,17].

Despite the interest for this tracer, ε_{Nd} sea water data are scarce, especially in the Pacific Ocean [5,18]. This is one of the reasons why the oceanic balance of Nd is not completely understood: the exact way according to which water masses change their Nd IC is still unclear, although exchanges with particulate material at the ocean margins and along the coasts are suspected to be likely candidates [7,8].

Coale et al. [46] reported Fe and Al maximum at the equator at 140°W in the Pacific Equatorial Undercurrent (EUC), between 100 and 250 m. As aeolian inputs are low in this area [19], Coale et al. [46] deduced that the iron found in the surface waters is supplied from the enriched subsurface layer by the equatorial upwelling. This input of iron could control the primary production in this region. These authors suggested that this iron may originate from the Papua New Guinea (PNG) shelf (or upper slope), and be advected within the EUC. Wells et al. [1] speculate that past variations in the tectonic activity of PNG (mostly during the late Miocene) could have induced variations of iron inputs into the EUC source waters and subsequently caused variations in the Central Equatorial Pacific primary production. It is therefore important to assess clearly the origin of the iron enrichment of the subsurface waters. The Nd isotopic signature of the PNG slope ($\varepsilon_{Nd} = +7$, [20]) is much more radiogenic (high ε_{Nd}) than the surrounding waters ($-9 < \varepsilon_{Nd} < 0$; [5]). Therefore, we expect that the Nd IC of the uppermost 1000 m in the Central Equatorial Pacific could help test whether the lithogenic enrichments measured by Coale et al. [46] indeed originate from the PNG.

2. Hydrological context and sampling

Within the framework of the EqPac cruise (*R.V. Thomson*, November 1992), 17 samples were collected at three stations, between the surface and 850 m depth, along a north–south transect (2°N to 12°S) around 140°W. Conductivity, temperature, depth (CTD) measurements were also carried out at those stations, as well as at intermediate stations.

The major features of the circulation of the surface Central Pacific Ocean are (i) two large anticyclonic gyres with axes along 20°N and 20°S and (ii) the equatorial current system (Fig. 1a). The northern limb of the southern anticyclonic gyre flows westwards and forms the South Equatorial Current (SEC), that extends from 5°N to 20°S at the surface. Below 100 m, the current shifts to the south and is found between 6°S and 25°S penetrating to depths greater than 1000 m [21] (Fig. 1b).

Along the equator, underneath the SEC, the EUC flows eastwards. This current originates north of PNG at ~200 m depth and rises gently along its 14 000 km pathway across the basin. It is located between 2°N and 2°S, is ~200 m thick, and has a mean speed of 0.4 m s^{-1} with a maximum around 1 m s^{-1} ([22,23] and compilation of current meter and ADCP (Acoustic Doppler Current Profiles) data from the TAO (Tropical Atmosphere Ocean) moorings (PMEL, US; JAMSTEC, Japan; IRD, France); Gourdeau, personal communication, 2000). It is mainly formed out of four undercurrents merging off the PNG coast (Fig. 1c). Three of them are coastal currents entraining waters of southern origin: the New Guinea Coastal Undercurrent (NGCU), the Saint Georges Undercurrent (SGU) and the New Ireland Coastal Undercurrent (NICU). The fourth one entrains waters of northern origin [24,25]. A strong pycnocline divides the EUC into two main layers: at 140°W, the upper one lies between 50 and 150 m and the lower one between 150 and 250 m. The upper layer includes the core of maximum velocity for the EUC. This layer contains Tropical Water originating from the high salinity cell centered around the tropic of Capricorn between 170°W and 120°W, where convective sinking of surface water takes place (Fig. 1a). This Tropical Water is entrained westwards in the SEC and then brought to the EUC by the coastal undercurrents described above. A large fraction of this water may be lost to the surface circulation as it flows eastwards [24]. The water that forms the subpycnocline layer of the EUC is described by Tsuchiya [26] as the Equatorial 13°C Water. Originating from the Tasman Sea, it flows eastwards to reach the southern limb of the south subtropical gyre, then it follows the course of this gyre, joining the SEC that brings it to the Coral Sea. Finally, it flows northwards to the Solomon Sea and enters the Bismarck Sea through the Vitiaz Strait in the NGCU from which it feeds the EUC [26] (Fig. 1a,c).

Underneath the EUC, the Equatorial Intermediate Current (EIC) flows westwards between ~3°N and ~2°S [22] and from about 300 to more than 500 m depth (Fig. 1b). Underneath the EIC the flow direction is eastwards again. The boundary between this eastwards flow and the EIC is uncertain but situated between 500 and 800 m depth [21]. On both sides of the EIC eastwards flows are found, the North and South Subsurface Countercurrents (NSCC and SSCC), about 5° wide each (Fig. 1b).

The intermediate water mass found at 135°W between 10°S and 6.5°N is described by Tsuchiya and Talley [34] as the Antarctic Intermediate Water (AAIW) of the 'equatorial type'. These authors suggest that it originates from the AAIW of the 'subtropical type' found between 33°S and 17°S. Following these authors, the AAIW of the subtropical type would be carried to the west by the SEC and then northwards to the equatorial zone by the western boundary undercurrents in the PNG region. Equatorial flows would then spread the water mass into the interior of the equatorial region. The region between 17°S and 10°S is an AAIW transition zone.

The samples collected during the EqPac cruise allow us to document some of these hydrographic structures along 140°W (Fig. 1b and Table 1 for hydrographical characteristics). At 12°S we have sampled at 120 and 150 m the tongue of Tropical Water formed by convective sinking ($S = 36.5$ and 36.4, respectively). At 200 m the sample is located around the path of the 13°C Equatorial Water. At 835 m, we have sampled in the transition zone for AAIW, adjacent to the equatorial type AAIW. At 0°, there are two samples in the core of the EUC: 120 and 150 m, one sample in the core of the EIC: 350 m, one in the bottom end of the EIC: 545 m and one sample of AAIW of the equatorial type at 835 m. The 2°N station is located at the northern limit of the equatorial upwelling. We collected a sample at 15 m in the SEC, a sample around the northern boundary of the EUC at

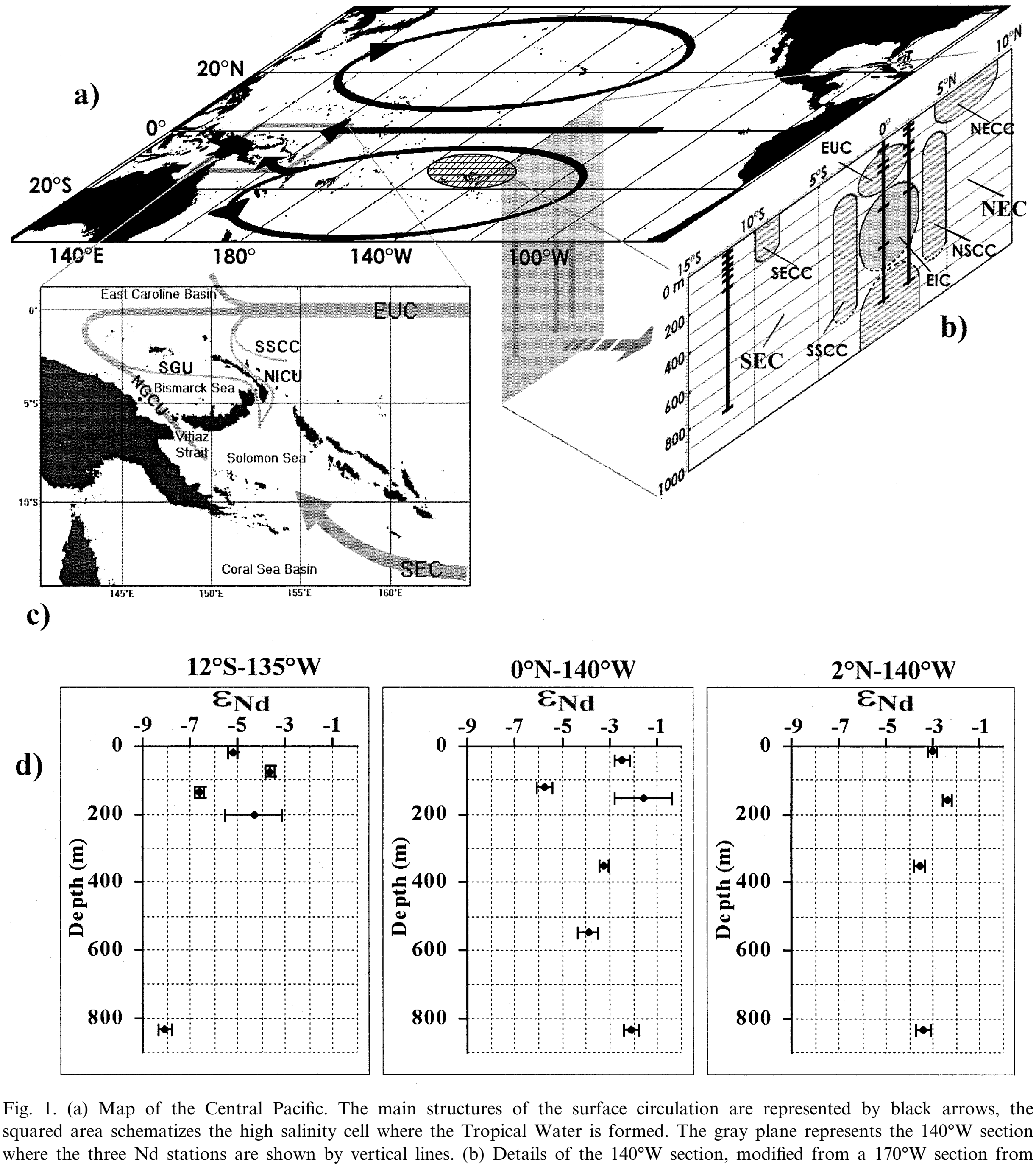

Fig. 1. (a) Map of the Central Pacific. The main structures of the surface circulation are represented by black arrows, the squared area schematizes the high salinity cell where the Tropical Water is formed. The gray plane represents the 140°W section where the three Nd stations are shown by vertical lines. (b) Details of the 140°W section, modified from a 170°W section from Tomczak and Godfrey [47]. The three stations are represented by the vertical black lines, on which the sample locations are shown by horizontal segments. The main zonal currents are schematized. Unfilled and gray tint areas are westward flows: the SEC, the North Equatorial Current (NEC), and the EIC. Striped areas are eastwards flows: the South Equatorial Counter Current (SECC), the North Equatorial Counter Current (NECC), the Southern Subsurface Counter Current (SSCC), the Northern Subsurface Counter Current (NSCC) and the EUC. Note that the bottom extensions of the SSCC, NSCC and EIC are not well defined in the literature (it is represented by a dotted line). (c) Zoom on the PNG region showing in detail the currents that form the EUC: The NGCU, the SGU, the NICU and the SSCC. (d) ε_{Nd} profiles at the three stations.

Table 1
Nd ICs, Ce anomalies and hydrological properties of the samples analyzed in this work

Station location	Depth (m)	θ (°C)	Salinity (psu)	σ_θ	Ce/Ce*	$^{143}Nd/^{144}Nd^a$	ε_{Nd}
2°N–140°W	15	26.246	34.582	22.643	0.51 ± 0.06	0.512484 ± 11	−3.0 ± 0.2
	40	26.239	34.582	22.645	0.36 ± 0.06	–	–
	110	22.817	34.730	23.783	0.37 ± 0.07	–	–
	155	13.978	34.910	26.123	0.17 ± 0.02	0.512516 ± 11	−2.3 ± 0.2
	350	11.011	34.776	26.599	0.32 ± 0.03	0.512455 ± 11	−3.5 ± 0.2
	835	5.401	34.548	27.270	0.23 ± 0.03	0.512463 ± 17	−3.4 ± 0.3
0°–140°W	40	24.598	34.954	23.430	0.34 ± 0.06	0.512511 ± 13	−2.4 ± 0.3
	120	19.674	35.134	24.950	0.33 ± 0.05	0.512343 ± 13	−5.7 ± 0.3
	150	17.236	35.174	25.593	0.26 ± 0.04	0.512556 ± 66	−1.6 ± 1.2
	350	10.847	34.783	26.635	0.21 ± 0.03	0.512471 ± 11	−3.2 ± 0.2
	545	7.823	34.620	27.002	0.54 ± 0.05	0.512437 ± 20	−3.9 ± 0.4
	835	4.341	34.549	27.278	0.22 ± 0.02	0.512530 ± 15	−2.1 ± 0.3
12°S–135°W	20	27.270	35.922	23.328	0.70 ± 0.07	0.512371 ± 11	−5.2 ± 0.2
	60	26.666	36.212	23.739	0.44 ± 0.06	–	–
	75 ± 15	26.269	36.345	23.966	–	0.512450 ± 11	−3.6 ± 0.2
	90	25.937	36.455	24.153	0.41 ± 0.08	–	–
	120	24.949	36.490	24.485	0.60 ± 0.07	–	–
	135 ± 15	24.124	36.467	24.717	–	0.512300 ± 11	−6.6 ± 0.2
	150	23.489	36.399	24.854	0.85 ± 0.10	–	–
	200	21.352	36.080	25.221	0.37 ± 0.06	0.512417 ± 66	−4.3 ± 1.2
	835	5.180	34.523	27.276	0.59 ± 0.05	0.512224 ± 16	−8.0 ± 0.3

–: not measured.
[a]Absolute errors of $^{143}Nd/^{144}Nd$ have to be multiplied by 10^{-6}.

155 m, a sample in the EIC at 350 m and a sample of AAIW of the equatorial type at 835 m.

3. Analytical procedures

3.1. Nd IC

The analytical procedure used to purify Nd from the sea water comprises three steps. First, 10 l of sea water were preconcentrated using C18 cartridges loaded with a REE complexant (HDEHP/H_2MEHP). The REE were subsequently eluted with 6 N HCl, which efficiently separated them from most sea water ions. This procedure is described in detail by Jeandel et al. [7]. Second, this solution is dried and dissolved in 2.5 N HCl for the separation of the REE from the remaining ions (traces of Ca, Sr, Ba, Mg...). This second extraction was a chromatography using a cationic resin [27]. The REE were eluted with 9 ml of 6 N HCl. This solution was dried and dissolved again in 0.3 N HCl for the final extraction of Nd. This last step is based on a reversed phase chromatography (anionic exchange; [6,28]).

Mass spectrometric analyses were carried out on a Finnigan MAT 261 mass spectrometer (static mode). Sample size for mass spectrometric analysis was typically 6–30 ng and Nd was analyzed as Nd^+. The $^{146}Nd/^{144}Nd$ ratio of 0.7219 is used to correct the mass fractionation. An international standard (La Jolla, $^{143}Nd/^{144}Nd = 0.511850 \pm 20 \times 10^{-6}$; Lugmair, personal communication, 2001) was analyzed daily ($n = 24$) to monitor instrumental drift. The averaged result was within the certified range of the La Jolla value, so that no instrumental bias had to be taken into account. The standard deviation of this average is 11×10^{-6} (2σ), that is 0.2 ε_{Nd} unit: this external precision was applied to all the results having a better counting statistic.

Blank values range between 120 and 300 pg, that is 2–5% of the signal. Our limited sampling did not allow us to split or duplicate any sample analyzed in this work: concentrations were too low and only one sample per depth was collected.

However, the procedure used here is exactly the same as the Jeandel et al. [7] procedure. We therefore expect a similar reproducibility, which is within the 2σ error of the counting statistics.

3.2. REE concentrations

REE concentrations were measured on a Perkin Elmer Elan 6000 Inductively Coupled Plasma Mass Spectrometer (ICP-MS), following the procedure established in our laboratory [17], which coupled an internal standard and an isotopic dilution analysis. First, REE concentrations were evaluated by comparing the machine responses for the sample and a standard solution. Then, isotopic dilution was applied to Nd and Yb only. This last method is independent of the analytical recovery. The comparison of the results obtained for Nd and Yb concentrations by both methods allows us to estimate the experiment recovery of these two elements in each sample (range of values: 77–100% and 87–100% for Nd and Yb, respectively). Efficiencies of the protocol for the other REE are calculated by linear interpolation; finally, their concentrations measured by the internal standard method were corrected. The weight of the samples was approximately known, inducing an uncertainty of about 20% on absolute concentration values. Nevertheless, this has no effect on the LREE/HREE ratio within a given sample, nor its Ce anomaly. Absolute values used in the discussion are from Zhang and Nozaki [15].

REE were extracted from sea water by iron oxide co-precipitation. A 0.5 l aliquot, first acidified to pH = 2, was spiked with ^{150}Nd (97.84%) and ^{172}Yb (94.9%). Then 1 ml of 1 N HNO_3 containing 0.5% Fe was added. After equilibration, the pH was increased to 7–8 by addition of NH_4OH, and co-precipitation took place. The REE–Fe precipitate was extracted by successive centrifugations. It was redissolved in 1 ml of 6 N HCl and loaded on an anion exchange column to remove Fe (0.8 cm in diameter, 4 cm in length, containing 2 ml Bio-Rad AG1×8 resin). REE were eluted with 9 ml of 6 N HCl. This solution was evaporated and the residue was redissolved in 9 ml of 0.3 N HNO_3 for ICP-MS measurement.

Concentrations were reproducible within 0.9% for LREE and 4% for HREE, the worse reproducibility corresponding to the smallest samples. Blank values were smaller than 40 pg for abundant LREE and 3 pg for HREE.

4. Results

4.1. Nd IC

The sea water Nd IC are reported in Table 1. Vertical profiles of ε_{Nd} are plotted on Fig. 1d.

4.1.1. 2°N–140°W

Vertical variations of ε_{Nd} values are quite small. ε_{Nd} values range from −3.5 to −2.3. The mean value is −3.1 ± 0.5. The AAIW sample (835 m) has a value of −3.4.

4.1.2. 0°–140°W

ε_{Nd} variations are much larger, ε_{Nd} values range from −5.7 to −1.6. The mean value is −3.2 ± 1.5. There is a very important difference (3.9 ε_{Nd} units) between the two samples of the EUC, only 30 m apart (120 and 150 m), but situated in two distinct layers of the undercurrent. The deepest one (150 m) has an isotopic value comparable to that observed for the same depth at 2°N. Measurements in the EIC gave values of −3.2 and −3.9, in the same range as that observed at 2°N for this current (ε_{Nd} = −3.5). The intermediate water sample at 835 m is relatively radiogenic, with a value of −2.1.

4.1.3. 12°S–135°W

Vertical variations of ε_{Nd} values are also significant, especially within the first 200 m. ε_{Nd} values are between −8.0 and −3.6. The average value is −5.5 ± 1.8, this is the least radiogenic station observed in this work. Because of the insufficient amount of Nd in some samples, we had to mix some of them to make one out of two. The 60 m and 90 m samples were mixed as well as the 120 m and 150 m ones, producing data at 75 ± 15 m and 135 ± 15 m, respectively. At 135 m, in the tongue of Tropical Water, ε_{Nd} is −6.6, whereas it is −4.3 at 200 m in the path of the Equatorial

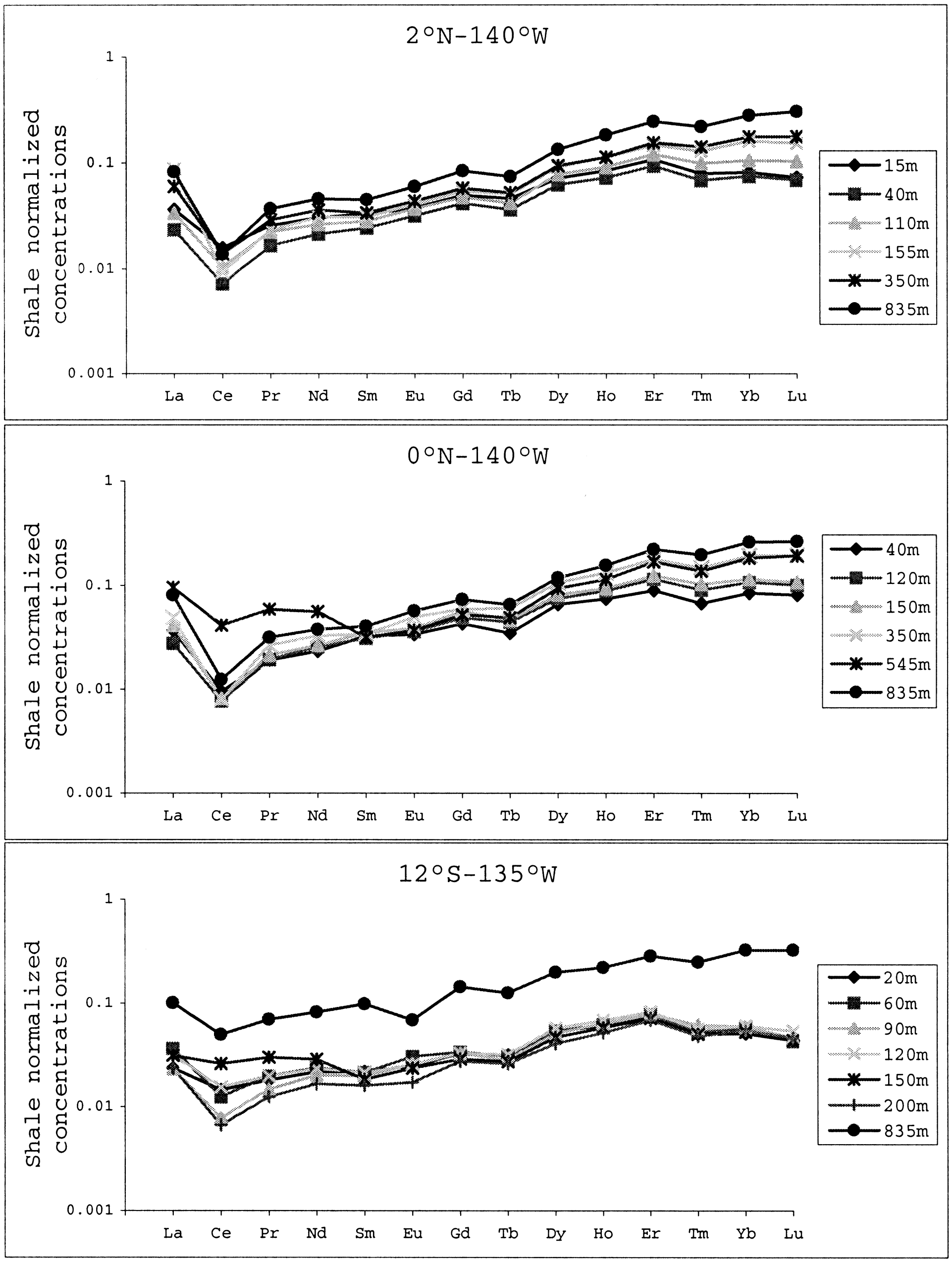

Fig. 2. Shale normalized REE concentrations of sea water samples collected during the EqPac cruise in November 1992. Due to the uncertainty affecting absolute concentrations of each sample (see the text), the shapes of the REE patterns are mostly used in this work.

13°C Water. The AAIW shows a value of −8.0, considerably less radiogenic than the intermediate waters of the two northernmost stations.

4.2. REE concentrations

REE patterns are shown in Fig. 2. Measured concentrations have been normalized to the average REE concentrations of North American, European and Russian shales ([16] and references therein). Patterns have marine properties, i.e. a negative cerium anomaly and a LREE/HREE fractionation. These characteristics reflect the particle activity and/or the aging during water mass transport: in general, the older (deeper) the water mass, the larger are the Ce anomaly and the HREE enrichment (e.g. [29]). In agreement with recent observations [19,30] surface waters do not reflect any influence of aeolian input at this remote longitude. Ce anomalies, Ce/Ce*, were calculated using the equation:

$$\frac{Ce}{Ce^*} = \frac{Ce \times 2}{(La + Pr)}$$

where Ce, La and Pr are the shale normalized concentrations (values close to 0 correspond to large anomalies whereas values close to 1 correspond to weak ones). Calculated anomalies are reported in Table 1. The most relevant features are the Ce anomalies of the three AAIW samples, which are 0.23 at 2°N, 0.22 at 0° and 0.59 at 12°S.

5. Discussion

Measured ε_{Nd} and REE concentrations are in good agreement with previous studies for the Pacific Ocean [3,5,18,29,31]. The average Nd IC of the whole Pacific basin is not significantly modified by our results ($\varepsilon_{Nd} = -4.3 \pm 1.8$ before our measurements to -4.2 ± 1.8 after). Similarly, the average ε_{Nd} shifts from -4.1 ± 1.5 to -4.0 ± 1.5 for the North Pacific and from -5.7 ± 3.7 to -5.6 ± 2.7 for the South Pacific. The measured value for AAIW at 12°S also compares well with preceding data [3,6,29], contrasting with the northernmost intermediate waters ('equatorial' AAIW) with its more radiogenic ε_{Nd} (Table 1, Fig. 1d). As a general rule, the 12°S station has a less radiogenic signature than the two others. This contrast can be related to the origins of the collected waters, the South Pacific being characterized by a less radiogenic signature than the North Pacific [5,18,32].

In the following, we will first discuss the Nd IC of the equatorial intermediate water (0° and 2°N), then that of the lower part of the EUC (0°, 150 m) and finally that of its upper part (0°, 120 m). In the three cases the results will be compared to the 12°S station results, since the latter can be considered as the origin of the waters found at the equator, as described by Tsuchiya ([24, 26,31]) and Tsuchiya and Talley [34] and represented on Fig. 1. The general picture is that part of the water entrained in the SEC (where the 12°S station is located) turns northwestwards towards PNG, and reaches the Central Equatorial Pacific (where the 0° and 2°N stations are located) entrained by equatorial flows. As the SEC is active to depths greater than 1000 m, it entrains the three layers studied here. The AAIW found at the equator comes from the South Subtropical Gyre by the way of western boundary undercurrents such as the NGCU, that flows northwestwards through the Vitiaz Strait and along the north coast of PNG [33,34]. The water found in the lower part of the EUC, originating from the Tasman Sea, flows around the South Subtropical Gyre before entering the NGCU, and finally reaches the EUC. The depth of the isopycnal characterizing this water ($\sigma_\theta = 26.4$) around the 12°S station is roughly 300 m [26]. At its source in the PNG region, the upper part of the EUC is mainly composed of waters originating on the high salinity cell centered around the tropic of Capricorn [24]. This tongue of high salinity was sampled at 135 m depth at the 12°S station. Note that all these trajectories involve western boundary coastal undercurrents of the PNG region.

5.1. Intermediate waters

Samples of intermediate waters at 2°N, 0° and 12°S show very similar hydrological properties (θ = 5.40, 5.34 and 5.18°C, S = 34.55, 34.55 and 34.52 psu, σ_θ = 27.27, 27.28 and 27.28 at 2°N, 0° and 12°S respectively, see Fig. 3). This indicates that they likely have a common origin, that is AAIW [34]. On the contrary, the measured Nd IC (Fig. 1d), and REE patterns (Fig. 2) are very similar at 2°N and 0° but there are large differences between these two stations and the 12°S one: ε_{Nd} increases from -8 ± 0.3 at 12°S,

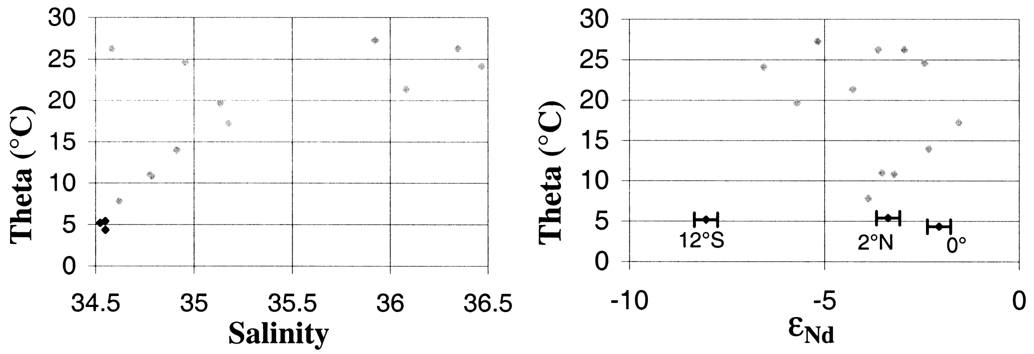

Fig. 3. θ-S and θ–ε_{Nd} diagrams of the analyzed samples. Black symbols represent AAIW samples. On the θ-S diagram AAIW show very similar characteristics, whereas they are clearly distinguishable on the θ–ε_{Nd} diagram.

to -2.1 ± 0.3 and -3.4 ± 0.3 at 0° and 2°N respectively. These significant ε_{Nd} variations contrast with the similar hydrographic properties, as illustrated in Fig. 3. Given that the Nd IC at 2°N and 0° are similar, we will consider only their average ($\varepsilon_{Nd}=-2.8\pm0.7$) in the following. As outlined above, such a radiogenic value in the northern part of the EqPac section requires that the AAIW found at 0°/2°N has been modified by an input of radiogenic Nd ($\varepsilon_{Nd}>-2.1$). The AAIW trajectory between 12°S and the equator through the PNG region (see above) offer one viable explanation for the ε_{Nd} variation from -8 in the 'southern' AAIW to -2.8 in the equatorial AAIW. Any ε_{Nd} change requires an input of Nd from a source with a different IC. Hydrography shows no mixing of water masses [34], which implies that the Nd input is of lithogenic origin. PNG (and adjacent volcanic islands) is the only land mass on the possible pathways of AAIW from the South Subtropical Gyre to the Equator. Its northeastern coast (together with the New Britain one, on the other side of the Vitiaz Strait) is characterized by $\varepsilon_{Nd\,PNG}\approx+7$ [20], a value radiogenic enough to allow the observed increase. In support of this, Jeandel et al. [7] suggested that the Nd isotopic signature of water masses is likely to be modified in areas where intense dissolved/particulate exchange occurs. This could happen in the vicinity of coasts, along continental slopes or within straits, where the hydrodynamics would enhance re-suspension of deposited sediment. The Vitiaz Strait is particularly narrow (less than 30 km width at 800 m depth) and is a likely place for changes in Nd IC in the waters flowing through it to occur. For these reasons we conclude that the AAIW isotopic signature is likely to be modified as it flows along the northern coast of PNG.

We now estimate the Nd fluxes required to achieve the observed ε_{Nd} variation through the Vitiaz Strait. The AAIW flows at about 2–4 Sv ([33]; 1 Sv $=10^6$ m^3 s^{-1}); we take here the average value ($F_1=3$ Sv). It flows at about 800 m depth, so that the Nd input might come from the PNG slope. The Nd concentrations measured in waters having AAIW properties (at 795 m in the Coral Sea, upstream from PNG and at 991 m in the Caroline Sea, downstream of PNG) are respectively $C_{up}=10$ pmol kg^{-1} and $C_{down}=9.3$ pmol kg^{-1} [15]. Neglecting the minor decrease, we assume that the Nd concentration is constant in this water mass as it flows along the coast of PNG. We assumed the upstream Nd IC to be that measured at 12°S ($\varepsilon_{Nd\,up}=-8$) and the downstream value to be the average of those measured at 2°N and 0° ($\varepsilon_{Nd\,down}=-2.8$). Constant concentrations combined with a varying ε_{Nd} requires an *exchange* of Nd between the slope of PNG and the AAIW. If E is the average flux of Nd exchanged and $\varepsilon_{Nd\,result}$ the Nd IC resulting from this process, then:

$$\varepsilon_{Nd\,result}=\frac{(C_{up}\times F_1-E)\times\varepsilon_{Nd\,up}+E\times\varepsilon_{Nd\,PNG}}{C_{down}\times F_1}\tag{1}$$

Taking $\varepsilon_{\mathrm{Nd\ PNG}} \approx +7$ [20], we find $E = 4.9\times10^7$ g(Nd) y^{-1}. The possible process causing this exchange of Nd between the slope of PNG and sea water will be discussed in detail in Section 5.2. However, we can estimate the amount of solid material that would be required to release the Nd contained in its lattice to obtain such fluxes, whatever the process. The Nd concentration in the volcanic PNG material is approximately 9 ppm [20], the percentage of dissolution of Nd from marine particles or sediments in sea water is between 3 and 20% [17,35,36]. Assuming an average of 10% dissolution, the amount of PNG material needed for this Nd exchange is 5.4×10^7 t y^{-1}, that is 9% of the fluvial sediment discharge from PNG to the ocean [37]. Milliman [37] demonstrated that this sediment discharged to an active margin directly reached the deep sea. The steepness of the slope likely induces re-suspension of the deposited material and favors solution/particles contact. The residence time of AAIW in the Vitiaz Strait is around 6 days; it reaches a maximum of 2 months when assuming that it flows along the whole slope of PNG in the NICU. This means an efficient modification of the water mass Nd signature in such an oceanographic context (strong hydrodynamics, high dissolved/particulate exchanges). These results are consistent with the more pronounced Ce anomaly in the 'equatorial type' AAIW: adsorption/desorption processes promote larger anomalies [17]. These results indicate that AAIW is modified from the 'southern type' to the 'equatorial type' by flowing along the PNG coast. They also confirm that the Nd isotope signature helps reconstruct the present-day pathways of a water mass even though its hydrographical properties are not strongly modified along its path (see Fig. 3 and [7]).

5.2. EUC

Two samples were analyzed in the core of the EUC at the equator. Despite their small difference in water depths, their Nd IC differ significantly ($\varepsilon_{\mathrm{Nd}} = -5.7\pm0.3$ at 120 m and $\varepsilon_{\mathrm{Nd}} = -1.6\pm1.2$ at 150 m). This indicates that the boundary between the two layers of the EUC is between those depths. The large vertical $\varepsilon_{\mathrm{Nd}}$ gradient also indicates that the two layers do not influence each other significantly. In other words, the upwelling does not seem to affect the subpycnocline layer of the EUC.

5.2.1. Lower part of the EUC

The lower part of the EUC comprises the 13°C Water. It is a thick and homogeneous layer, not directly involved in the Ekman flow [24] so that, to a first approximation, we assume that its Nd IC remains constant between the source of the EUC and the 140°W section ($\varepsilon_{\mathrm{Nd}} = -1.6\pm1.2$). The Nd IC of the 13°C Water entering the NGCU was chosen to be that of our 12°S sample having the closest density to that characterizing the 13°C Water ($\varepsilon_{\mathrm{Nd}} = -4.3\pm1.2$, 200 m). These hypotheses suggest an increase from $\varepsilon_{\mathrm{Nd}} = -4.3$ to $\varepsilon_{\mathrm{Nd}} = -1.6$ while the water flows in the NGCU. The concentrations measured by Zhang and Nozaki [15] in the Coral and Caroline Sea for the layer with the density of the 13°C Water ($\sigma_\theta = 26.4$) show a slight increase: $C_{\mathrm{up}} = 4.9$ pmol kg^{-1} and $C_{\mathrm{down}} = 6.6$ pmol kg^{-1} respectively. The flux of the 13°C Water is estimated at $F_2 = 3$ Sv from data given by Lindstrom et al. [38]. The concentration increase (1.7 pmol l^{-1}) in this layer requires an input of Nd from PNG of 2.3×10^7 g(Nd) y^{-1}. With the 13°C Waters flowing around 300 m depth, Nd inputs are likely to be provided by the PNG the upper slope. This input modifies $\varepsilon_{\mathrm{Nd}}$ as follows:

$$\varepsilon_{\mathrm{Nd\ result}} = \frac{C_{\mathrm{up}}\times F_2\times\varepsilon_{\mathrm{Nd\ up}} + (C_{\mathrm{down}}-C_{\mathrm{up}})\times F_2\times\varepsilon_{\mathrm{Nd\ PNG}}}{C_{\mathrm{down}}\times F_2} \tag{2}$$

The resulting Nd IC is $\varepsilon_{\mathrm{Nd\ result}} = -1.4$, very close to the measured value of -1.6. No exchange is required this time to reconcile the concentration and isotopic signal variations. This input of Nd roughly corresponds to the remobilization of 2.6×10^7 t y^{-1} of PNG material, that is 4% of the total fluvial load [37]. This small proportion is of the same order as above, and makes our explanation conceivable.

The fact that exchange processes are required to explain the variations observed in the AAIW and not in the 13°C layer can be related to (1) different speciations of Nd in the different input sources or (2) velocity differences between the currents entraining the 13°C Water and the AAIW (about 70 cm s^{-1} and 12 cm s^{-1}, respectively [33,38]). However this difference of behavior could not be significant because we initially assumed no ε_{Nd} variation within the EUC. However, the salinity at 0° 150 m is 35.17 whereas the same isopycnal leaves the PNG region with a value 35.5. This slight freshening could reflect the merging of waters originating from the Northern Pacific into the EUC, although the precise dynamic of this input is not yet understood [24]. From the literature [5] and this work, the Nd IC of these waters is likely below −1.6. If this input occurs, it would therefore induce a decrease of ε_{Nd} between PNG and 140°W, implying that waters would leave the PNG with a more radiogenic value than that assumed here ($\varepsilon_{Nd} = -1.6$). In that case, the ε_{Nd} increase in the NGCU could no longer be explained by a sole input, an exchange would become necessary. The lack of ε_{Nd} data in the PNG region does not allow us to conclude firmly on that point, the hypothesis of a sole input remaining the most probable hypothesis regarding our data set.

Three kinds of sources can be considered to explain the input: (1) Hydrothermal inputs seem unlikely since it has been demonstrated that the influence of hydrothermalism is not significant for the local and global REE budget in the ocean [39]. (2) Dissolved riverine inputs: following Sholkovitz et al. [16], the europium weathered from PNG as dissolved load explains 20% of the excess of the Eu observed in the upper layers of the Caroline Sea. Using their data, we estimated that about 1.9×10^6 g y^{-1} of dissolved riverine Nd are brought to the upper Caroline Sea, that is less than 10% of the amount required to explain the Nd enrichment and the isotopic variation. In addition, Sholkovitz (personal communication, 2000) provided us with the only dissolved Nd IC measured in the SEPIK river. Its ε_{Nd} is −3.1, definitely more negative than the volcanic material outcropping on the eastern coast (about +7; [20]). Finally, Sholkovitz et al. [16] suggested that the dissolved riverine REE inputs from PNG can be traced in the surface layers of the Caroline Sea by a mid-REE enrichment when the samples are normalized to a composite reference, deduced from the Coral Sea data of Zhang and Nozaki [15]. We applied this normalization to all our REE patterns, and did not observe any mid-REE enrichment between the southern and northern stations of the section. Hence, we suspect that direct input of riverine dissolved Nd plays a minor role in the variations observed. (3) The best candidate is the dissolution of solid material at the continent/ocean interface (shelf, slope...). This process can yield the two types of behaviors, exchange or net input, but does not give a hint which one to favor. This third hypothesis is also invoked to explain 80% of the Eu excess observed in the upper layers of the Caroline Sea, the excess which is not balanced by dissolved riverine [16]. This 'exchange' hypothesis has previously been proposed to reconcile the variations of Nd concentration and Nd IC on a basin scale [6,7] and on a global scale [9,29]. Although it would be useful to quantify this process here, we demonstrated above that our data do not allow to solve that point here. However, the Nd isotope signal does demonstrate what was suspected [40]: that lithogenic elements are transported across the Pacific Ocean within the subpycnocline layer of the EUC and that they originate from PNG.

This westward advection of lithogenic material is supported by the high ^{228}Ra signal observed in subsurface waters collected at the same location as this study, but earlier in the year (spring 1992; [41]). The strong ^{228}Ra gradient also supports the idea that the equatorial upwelling does not affect the 13°C layer. Ku et al. [41] suggested that the source of ^{228}Ra is the nearby western American coast. We do not agree with this interpretation as (1) the ε_{Nd} of Californian inputs is expected to be around −5 [42], which is too low to explain the equatorial ε_{Nd} values and (2) the hydrographic literature clearly states that advection is eastwards for these waters.

5.2.2. Upper part of the EUC

The upper part of the EUC, containing Tropical Waters, is affected by equatorial upwelling and lateral advection. Thus, a large part of its water is renewed on its way from the PNG coast to 140°W [24]. Wells et al. [1] proposed a simple model of this layer to explain the dissolved Fe concentrations measured at 140°W in the EUC: 0.1 nmol kg^{-1} in the upper part and 0.35 nmol kg^{-1} in the lower part. These authors assumed that both layers have the same iron concentration (0.35 nmol kg^{-1}) when leaving the PNG coast, the lower layer remaining unchanged all the way to 140°W. On the contrary, the upper part loses Fe by upwelling, while no enrichment occurs by lateral advection since the surrounding waters are Fe-depleted. This results in an exponential decrease of the dissolved Fe concentration from 0.35 to 0.1 nmol kg^{-1} at 140°W [1]. This model was modified to reconstruct the variation of the Nd IC along the upper layer of the EUC. First, we took into account lateral inputs, since surrounding waters are not Nd-depleted. In addition we considered that the horizontal velocity of the EUC is 0.4 m s^{-1} instead of the 1 m s^{-1} taken by Wells et al. [1]. The former estimate was made for the period of about 6 months that effectively corresponds to the transport of the water that was sampled at 140°W in November 1992. Four different sources of data converge towards this lower value: (1) The TAO ADCP and current meter data at the equator, at 165°E, 170°W and 140°W gave velocities between 0.4 and 0.8 m s^{-1}; but these values overestimate the average EUC current speed since they sample its maximum velocity. (2) Wyrtki and Kilonsky [22] give the mean transport and area of the EUC measured during the Hawaii-to-Tahiti Shuttle Experiment (1979–1980, around 155°W) from which we calculated a mean velocity of 0.4 m s^{-1}. (3) From a depth profile of a modeled zonal velocity averaged over the period from 1992 to 1997 at 0°–140°W [43], we calculated a mean velocity of 0.6 m s^{-1}, likely to be overestimated because centered on the equator, as for the TAO data. (4) Finally, Gourdeau (personal communication, 2000), using the model from Gent and Cane [44], gave us the zonal velocity averaged between 2.2°N and 2.2°S, for the 6 months preceding the sampling. From those simulations we extracted a mean zonal velocity of 0.4 m s^{-1} in the EUC. We therefore adopted 0.4 m s^{-1}.

Then, we estimated the Nd IC in the upper EUC layer at its source. As it has neither the same origin, nor the same volume as the underlying 13°C layer, we cannot assume that it has the same Nd signal when leaving PNG. In its formation region it is characterized by $\varepsilon_{\mathrm{Nd\ up}} = -6.6$ (12°S, 135 m). We assumed then that this Tropical Water flowing through the Vitiaz Strait interacts with the PNG upper slope in a similar way to the 13°C Water, i.e. that there is no Nd exchange, only inputs. This assumption is based on the facts that these two water masses are flowing on top of each other in the NGCU (150–200 m and 220–360 m for the Tropical Water and the 13°C Water, respectively); therefore they should interact with similar layers along the slope; in addition, their speeds are close to each other (around 90 cm s^{-1} and 70 cm s^{-1} respectively). The flux of Tropical Water through the Vitiaz Strait is estimated to be 2 Sv [38]. The concentrations upstream and downstream of PNG are those of Zhang and Nozaki [15] in the Coral and Caroline Sea, $C_{\mathrm{up}} = 3.5$ pmol kg^{-1} and $C_{\mathrm{down}} = 4.25$ pmol kg^{-1} respectively. The values are chosen at $\sigma_\theta = 24.95$, which is the density of the Tropical Water in that area. Applying Eq. 2 to these data, we find $\varepsilon_{\mathrm{Nd\ down}} = -4.2$. This value will be used as the starting value in the following model.

The model is sketched on Fig. 4. The upper layer of the EUC is represented as a rectangular box, 8333 km long (from 145°E to 140°W) and 100 m thick (50–150 m). The horizontal velocity is constant and set to 0.4 m s^{-1}, the vertical velocity is also constant and set to 1.23 m day^{-1} [45]. This implies a water renewal of approximately 95% between the source of the EUC and 140°W. This renewal corresponds to a loss from the top due to upwelling and to a gain from the side due to lateral advection. The proportions of water advected from the northern and southern sides of the box are constrained by the salinity budget (Fig. 4). Salinity values used for lateral inputs were those measured during the campaign at 2°N and 2°S at 120 m depth (34.8 and 35.2 respectively). The original salinity value of the Tropical Water in the region of formation of the

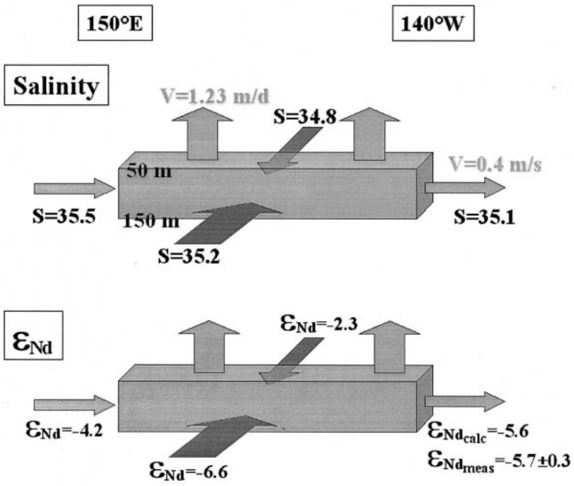

Fig. 4. Model of the upper layer of the EUC, between 150°E and 140°W. The velocity of the westward flow is set to 0.4 m s^{-1}, the one of the upwelling to 1.23 m day^{-1}. Lateral advection is constrained by salinity. The model is then used to calculate ε_{Nd} at 140°W from ε_{Nd} values at the source (150°E) and in the advected waters.

EUC is that given by Tsuchiya et al. ([24]; $S = 35.5$). This constraint implies that out of the 95% of water renewal, 74% came from the south and 21% from the north. We assumed a constant and equal Nd concentration inside and outside the box (this work). The Nd IC for the water advected from the south is set at $\varepsilon_{Nd\ south} = -6.6$ because this is the value of the Tropical Water measured at 12°S. The Nd IC for the water advected from the north is set to $\varepsilon_{Nd\ north} = -2.3$, as measured at the level corresponding to the upper layer of the EUC at 2°N, that is 155 m. The output of the model gives a Nd IC at 140°W in the upper layer of the EUC of −5.6, perfectly consistent with the measured value of -5.7 ± 0.3 for this layer. Owing to the hypothesis made for the ε_{Nd} value for the upper EUC waters at their origin, this agreement has to be considered with caution. Nevertheless, the good agreement between measured and calculated values also holds when a horizontal velocity of 1 m s^{-1} is applied to this model [1]: this corresponds to a renewal of 70% of the water, and yields a calculated ε_{Nd} value of −5, only slightly below the measured one. We also tested the sensitivity of our calculation to the original ε_{Nd} value taken at 12°S: assuming that it is of −3.6, as measured at 12°S, 75 m, the ε_{Nd} value after the PNG would be −1.7 and the resulting ε_{Nd} value after the renewal of waters at 140°W would be −5.5. In any case, the original value of the Tropical water is not crucial for the remaining calculation: the renewal of waters due to the active equatorial upwelling suppresses any PNG contribution on these surface waters. On the other hand, applying a velocity of 0.4 m s^{-1} to calculate the iron concentration variations leads to the total depletion of iron in the surface layer of 140°W, with a calculated value of 0.02 pmol l^{-1}, far below the measured one [46].

Wells et al. [1] suggest that paleo-variations in primary production in the eastern Equatorial Pacific could reflect variations in the tectonic activity of PNG. Such activity would imply variations in the Fe enrichment of the source waters of the EUC and therefore variations of the Fe content of the surface waters of the eastern Equatorial Pacific. Primary production being limited by Fe in this area [46], this would result in variations in the primary production. Our results contradict this hypothesis, as the important renewal of the upper layer of the EUC (due to upwelling) seems to completely eliminate the PNG imprint, as shown by the depletion of the Nd signal in this layer. This would have a similar effect on iron. On the other hand, neither the Fe nor the ε_{Nd} of this water is known at its source today (both are estimated in [1] and this work). In addition, all these hypotheses assume that the mean upwelling conditions today were the same as those in the past, which are not known. Higher Fe contents and/or more radiogenic ε_{Nd} values could yield a remaining signal at 140°W, even after water renewal: ε_{Nd} measurements of sediments deposited during higher productivity events would certainly help to solve these questions.

6. Conclusion

We characterized the Nd IC of hydrodynamic structures in the Equatorial Pacific Ocean at 140°W: Intermediate Water at 12°S: $\varepsilon_{Nd} = -8.0 \pm 0.3$; Intermediate Water of the equatorial type: $\varepsilon_{Nd} = -2.8 \pm 0.7$; Upper layer of the EUC: $\varepsilon_{Nd} = -5.7 \pm 0.3$; Subpycnocline layer of the EUC: $\varepsilon_{Nd} = -1.6 \pm 1.2$; EIC: $\varepsilon_{Nd} = -3.5 \pm 0.4$; Tropical Water formed in the high salinity cell of the Tropic of Capricorn: $\varepsilon_{Nd} = -6.6 \pm 0.2$

The Nd IC of the three Intermediate Water samples confirm the hypothesis proposed by Tsuchiya and Talley [34]: the Intermediate Water found at 140°W in the equatorial region is a 'modified AAIW' and comes from the South Subtropical Gyre by the way of the western boundary undercurrents. Whereas its hydrological properties remain unchanged, its Nd signature is strongly modified by the contact with the PNG slope, confirming the usefulness of this tracer to identify the pathway of water masses.

The Nd IC measured in the subpycnocline layer of the EUC at 140°W ($\varepsilon_{Nd} = -1.6 \pm 1.2$, 150 m) also reflects the influence of PNG lithogenic inputs on the Central Equatorial Pacific. This emphasizes the importance of jets to transport lithogenic material into the subsurface layers of basin centers, where aeolian inputs are particularly weak. This corroborates the preceding results on Fe and Al maxima in this area [1].

The Nd IC of the upper layer of the EUC ($\varepsilon_{Nd} = -5.7 \pm 0.3$, 120 m) is very different from that of the subpycnocline layer ($\varepsilon_{Nd} = -1.6 \pm 1.2$, 150 m) indicating that upwelling was not active between 150 and 120 m at the place and time of the sampling. A simple model of the upper layer of the EUC, with an average velocity lowered to 60% from the Wells value, shows that the radiogenic Nd enrichment originating from PNG (and therefore Fe enrichment) likely disappears from this layer as it traverses the basin. For these two reasons we suspect that PNG lithogenic inputs were not able to affect the surface water of the Central Equatorial Pacific, as suggested by Wells et al. [1]. However, this contradiction may be due to (i) the simplicity of both Wells' and our models, (ii) the lack of ε_{Nd} and Fe data in the source of EUC (PNG area) and therefore uncertainties on these supposed values.

Our best candidate to explain REE inputs in intermediate and subsurface waters in this area is the dissolution of volcanogenic material, supplied by erosion, caused by boundary undercurrents flowing against the PNG slope. This process is the same as the one suggested by Wells et al. [1] for the iron inputs. Therefore, we suppose that Fe and REE enrichments are tightly linked. This is why, if measurements of traditional paleo-primary production tracers are made in the sediment of the Central Equatorial Pacific to identify past input variations, it would be essential to measure also the authigenic Nd isotopic signatures imprinted in the sediments.

Acknowledgements

Marty Fleisher is deeply thanked for having collected the samples during the EqPac cruise of November 1992. We acknowledge also Margaret Leinen, chief scientist, for having accepted this additional sampling during the cruise, as well as the captain and the crew of the *R.V. Thomson*. We also thank D. Yeghicheyan, K. Tachikawa, M. Roy-Barman, F. Candaudap, M. Souhaut, P. Brunet, M. Valladon and B. Reynier for their analytical and technical support during F. Lacan's master training period. Comments of M. Rutgers Van der Loeff, V. Athias and R. Morrow, as well as the constructive reviews of D. Vance, M. Frank and an anonymous reviewer, considerably helped to improve this manuscript. ***[AH]***

References

[1] M.L. Wells, G.K. Vallis, E.A. Silver, Tectonic processes in Papua New Guinea and past productivity in the eastern Equatorial Pacific Ocean, Nature 398 (1999) 601–604.

[2] S.B. Jacobsen, G.J. Wasserburg, Sm–Nd isotopic evolution of chondrites, Earth Planet. Sci. Lett. 50 (1980) 139–155.

[3] D.J. Piepgras, G.J. Wasserburg, Isotopic composition of neodymium in waters from the Drake Passage, Science 217 (1982) 207–217.

[4] D.J. Piepgras, G.J. Wasserburg, Rare Earth Element transport in the western North Atlantic inferred from isotopic observations, Geochim. Cosmochim. Acta 51 (1987) 1257–1271.

[5] D.J. Piepgras, S.B. Jacobsen, The isotopic composition of neodymium in the North Pacific, Geochim. Cosmochim. Acta 52 (1988) 1373–1381.

[6] C. Jeandel, Concentration and isotopic composition of neodymium in the South Atlantic Ocean, Earth Planet. Sci. Lett. 117 (1993) 581–591.

[7] C. Jeandel, D. Thouron, M. Fieux, Concentrations and Isotopic compositions of Nd in the Eastern Indian Ocean and Indonesian Straits, Geochim. Cosmochim. Acta 62 (1998) 2597–2607.

[8] H. Amakawa, D.S. Alibo, Y. Nozaki, Nd isotopic and REE pattern in the surface waters of the eastern Indian Ocean and its adjacent seas, Geochim. Cosmochim. Acta 64 (2000) 1715–1727.

[9] K. Tachikawa, V. Athias, C. Jeandel, The Neodymium paradox in the ocean, J. Geophys. Res., submitted.

[10] C. Jeandel, J.K. Bishop, A. Zindler, Exchange of Nd and its isotopes between seawater small and large particles in the Sargasso Sea, Geochim. Cosmochim. Acta 59 (1995) 535–547.

[11] F.E. Grousset, M. Parra, A. Bory, P. Martinez, P. Bertrand, G. Shimmield, R.M. Ellam, Saharan wind regimes traced by the Sr–Nd isotopic compositions of the subtropical Atlantic sediments: last glacial maximum vs. today, Q. Sci. Rev. 17 (1998) 395–409.

[12] F. Henry, C. Jeandel, J.-F. Minster, Particulate and dissolved Nd in the Western Mediterranean Sea: sources, fates and budget, Mar. Chem. 45 (1994) 283–305.

[13] K. Tachikawa, C. Jeandel, A. Vangriesheim, B. Dupré, Distribution of Rare Earth Elements and neodymium isotopes in suspended particles of the tropical Atlantic Ocean (EUMELI site), Deep-Sea Res. 46 (1999) 733–756.

[14] H. Elderfield, The oceanic chemistry of the Rare Earth Elements, Phil. Trans. R. Soc. Lond. 325 (1988) 105–106.

[15] J. Zhang, Y. Nozaki, Rare Earth Elements and yttrium in seawater: ICP-MS determinations in the East Caroline, Coral Sea and South Fiji basins of the western south Pacific Ocean, Geochim. Cosmochim. Acta 60 (1996) 4631–4644.

[16] E.R. Sholkovitz, H. Elderfield, R. Szymczak, K. Casey, Island weathering: river sources of Rare Earth Elements to the Western Pacific Ocean, Mar. Chem. 68 (1999) 39–57.

[17] K. Tachikawa, C. Jeandel, M. Roy-Barman, A new approach to Nd residence time in the ocean: the role of atmospheric inputs, Earth Planet. Sci. Lett. 170 (1999) 433–446.

[18] H. Shimizu, K. Tachikawa, A. Masuda, Y. Nozaki, Cerium and neodymium ratios and REE patterns in seawater from the North Pacific Ocean, Geochim. Cosmochim. Acta 58 (1994) 323–333.

[19] R.A. Duce, P.S. Liss, J.T. Merrill, E.L. Atlas, P. Buat-Ménard, B.B. Hicks, J.M. Miller, J.M. Prospero, R. Arimoto, T.M. Church, W. Ellis, J.N. Galloway, L. Hansen, T.D. Jickells, A.H. Knap, K.H. Reinhardt, B. Schneider, A. Soudine, J.J. Tokos, S. Tsunogai, R. Wollast, M. Zhou, The atmospheric input of trace species to the world ocean, Glob. Biogeochem. Cycles 5 (1991) 193–259.

[20] J.B. Gill, J.D. Morris, R.W. Johnson, Timescale for producing the geochemical signature of island arc magmas: U–Th–Po and Be–B systematics in recent Papua New Guinea lavas, Geochim. Cosmochim. Acta 57 (1993) 4269–4283.

[21] J.L. Reid, On the total geostrophic circulation of the pacific ocean: flow patterns, tracers, and transports, Prog. Oceanogr. 39 (1997) 236–352.

[22] K. Wyrtki, B. Kilonsky, Mean water and current structure during the Hawaii-to-Tahiti shuttle experiment, J. Phys. Oceanogr. 14 (1984) 242–254.

[23] R. Lukas, E. Firing, The geostrophic balance of the Pacific Equatorial Undercurrent, Deep-Sea Res. 31 (1984) 61–66.

[24] M. Tsuchiya, R. Lukas, R.A. Fine, Source Waters of the Pacific Equatorial Undercurrent, Prog. Oceanogr. 23 (1989) 101–147.

[25] J. Butt, E. Lindstrom, Currents off the east coast of New Ireland, Papua New Guinea, and their relevance to regional undercurrents in the Western Equatorial Pacific Ocean, J. Geophys. Res. 99 (1999) 12503–12514.

[26] M. Tsuchiya, The Origin of the Pacific Equatorial 13°C Water, J. Phys. Oceanogr. 11 (1981) 794–812.

[27] M. Loubet, Géochimie des Terres Rares dans les massifs de péridotites dits de 'haute température'. Evolution du manteau terrestre, Ph.D., Paris VII, 1976.

[28] P. Richard, N. Shimizu, C.J. Allègre, $^{143}Nd/^{146}Nd$, a natural tracer: an application to oceanic basalts, Earth Planet. Sci. Lett. 31 (1976) 269–278.

[29] C.J. Bertram, H. Elderfield, The geochemical balance of the Rare Earth Elements and Nd isotopes in the oceans, Geochim. Cosmochim. Acta 57 (1993) 1957–1986.

[30] M.J. Greaves, H. Elderfield, E.R. Sholkovitz, Aeolian sources of Rare Earth Elements to the Western Pacific Ocean, Mar. Chem. 68 (1999) 31–38.

[31] D.J. Piepgras, G.J. Wasserburg, E.G. Dasch, The isotopic composition of Nd in different ocean masses, Earth Planet. Sci. Lett. 45 (1979) 223–236.

[32] A. Aplin, A. Michard, F. Albarede, $^{143}Nd/^{144}Nd$ in Pacific ferromanganese incrustations and nodules, Earth Planet. Sci. Lett. 81 (1986) 7–14.

[33] M. Tsuchiya, Flow path of the Antarctic Intermediate Water in the western equatorial South Pacific Ocean, Deep-Sea Res. 38 (Suppl. 1) (1991) S273–S279.

[34] M. Tsuchiya, L.D. Talley, Water-property distributions along an eastern Pacific hydrographic section at 135°W, J. Mar. Res. 54 (1996) 541–564.

[35] R. Arraes-Mescoff, L. Coppola, M. Roy-Barman, M. Souhaut, K. Tachikawa, C. Jeandel, R. Sempéré, C. Yoro, The behavior of Al, Mn, Ba, Sr, REE and Th isotopes during in vitro bacterial degradation of large marine particles, Mar. Chem., in press.

[36] M.J. Greaves, P.J. Statham, H. Elderfield, Rare Earth Element mobilization from marine atmospheric dust into seawater, Mar. Chem. 46 (1994) 255–260.

[37] J.D. Milliman, Sediment discharge to the ocean from mountainous rivers: the New Guinea example, Geo-Mar. Lett. 15 (1995) 127–133.

[38] E. Lindstrom, J. Butt, R. Lukas, S. Godfrey, The flow

through Vitiaz Strait and St. George's channel, Papua New Guinea, The physical Oceanography of Sea Straits, 1990, pp. 171–189.

[39] A. Michard, F. Albarède, G. Michard, J.F. Minster, J.L. Charlou, Rare Earth Elements and uranium in high-temperature solutions from East Pacific Rise hydrothermal vent field (13°N), Nature 303 (1983) 795–797.

[40] A.L. Gordon, H.W. Taylor, D.T. Georgi, Antarctic oceanographic zonation, in: Polar Oceans Conference, M.J. Dunbar, 1977, pp. 45–76.

[41] T.L. Ku, S. Luo, M. Kusakabe, J.K.B. Bishop, ^{228}Ra-derived nutrient budgets in the upper Equatorial Pacific and the role of 'new' silicate in limiting productivity, Deep-Sea Res. 42 (1995) 479–497.

[42] S.L. Goldstein, S.B. Jacobsen, The Nd and Sr isotopic systematics of river-water dissolved material: implications for the sources of Nd and Sr in the seawater, Chem. Geol. Isot. Geosc. Sect. 66 (1987) 245–272.

[43] H.F. Seidel, B.S. Giese, Equatorial currents in the Pacific Ocean 1992–1997, J. Geophys. Res. 104 (1999) 7849–7863.

[44] P.R. Gent, M.A. Cane, A reduced gravity primitive equation model of the upper equatorial ocean, J. Comput. Phys. 81 (1989) 444–480.

[45] H.L. Bryden, E.C. Brady, Diagnostic model of the three-dimensional circulation in the upper Equatorial Pacific Ocean, J. Phys. Oceanogr. 15 (1985) 1255–1273.

[46] K.H. Coale, S.E. Fitzwater, R.M. Gordon, K.S. Johnson, R.T. Barber, Control of community growth and export production by upwelled iron in the Equatorial Pacific Ocean, Nature 379 (1996) 621–624.

[47] M. Tomczak, J.S. Godfrey, Regional Oceanography: An Introduction, Pergamon, Oxford, 1994, 422 pp.